macol., **16**, 1941 (1967).
(19) D. F. DeTar and M. N. Turetyky, *J. Am. Chem. Soc.*, **77**, 1745 (1955).
(20) K. Omura and T. Matsura, *Tetrahedron*, **26**, 255 (1970).
(21) B. D. Andresen, J. L. Templeton, R. H. Hammer, and H. L. Panzik, *Res. Commun. Chem. Pathol. Pharmacol.*, **14**, 259 (1976).
(22) E. Tegmann, E. Sury, and K. Hoffmann, *Helv. Chim. Acta*, **35**, 1235 (1952).
(23) S. Kukolja, D. Grguric, and L. Lopina, *Croat. Chem. Acta*, **33**, 41 (1961).
(24) E. von Kovates, *Helv. Chim. Acta*, **41**, 1915 (1958).
(25) B. D. Andresen, F. T. Davis, J. L. Templeton, R. H. Hammer, and H. L. Panzik, *Res. Commun. Chem. Pathol. Pharmacol.*, **15**, 21 (1976).
(26) B. D. Andresen, F. T. Davis, J. L. Templeton, H. L. Panzik, and R. H. Hammer, *ibid.*, **18**, 439 (1977).

ACKNOWLEDGMENTS

Supported in part by a Cottrell Starter Grant administered by Research Corporation.

The authors thank Dr. Harold L. Panzik and Mr. James L. Templeton for assistance.

Hydrolysis and Dissolution Behavior of a Prolonged-Release Prodrug of Theophylline: 7,7′-Succinylditheophylline

H. K. LEE *x, H. LAMBERT *, V. J. STELLA ‡, D. WANG ‡, and T. HIGUCHI ‡

Received June 14, 1978, from **Pharmaceutical Research and Development, Searle Laboratories, Skokie, IL 60076*, and the ‡*Department of Pharmaceutical Chemistry, University of Kansas, Lawrence, KS 66045.* Accepted for publication August 11, 1978.

Abstract □ The physicochemical characteristics of 7,7′-succinylditheophylline, a slow dissolving prodrug of theophylline, were investigated at 25°. One molecule of 7,7′-succinylditheophylline hydrolyzed to give two molecules of theophylline and one molecule of succinic acid. At 25° in aqueous solution, constant ionic strength, and zero buffer concentration, the pH profile for the hydrolysis of 7,7′-succinylditheophylline could be described adequately by a spontaneous constant, k_0, of 8.15×10^{-2} sec^{-1} and a hydroxide catalytic constant, k_{OH^-}, of 1.46×10^5 M^{-1} sec^{-1}. No specific acid catalysis was seen at pH values as low as 1. This dissolution rate of 7,7′-succinylditheophylline from a constant surface area pellet was independent of pH below 8. However, at pH values greater than 8, the dissolution rate was accelerated by a base. This behavior was consistent with the dissolution rate being catalyzed by the simultaneous chemical reaction of 7,7′-succinylditheophylline with hydroxide ion at a rate such that substantial hydrolysis of the substrate was occurring in the dissolution film. Dissolution with simultaneous chemical reaction for 7,7′-succinylditheophylline was analyzed theoretically on the basis of a film theory model. Excellent correlation between the theoretical and observed dissolution behavior was found. At pH values less than 8, the dissolution of 7,7′-succinylditheophylline was 35 times slower than that of theophylline. Based on this result, the aqueous solubility of 7,7′-succinylditheophylline was estimated to be 1.63×10^{-3} M.

Keyphrases □ 7,7′-Succinylditheophylline—hydrolysis and dissolution, effect of pH □ Prodrugs, theophylline—7,7′-succinylditheophylline, hydrolysis and dissolution, effect of pH □ Hydrolysis—7,7′-succinylditheophylline, effect of pH □ Dissolution—7,7′-succinylditheophylline, effect of pH □ Theophylline prodrugs—7,7′-succinylditheophylline, hydrolysis and dissolution, effect of pH

Theophylline is an effective bronchodilator used widely for the treatment of asthma. The improvement of pulmonary function in asthmatic patients was related to the plasma theophylline concentration (1–4). An optimal serum concentration range of 10–20 μg/ml was reported (5), although ranges from 5 to 20 μg/ml are often quoted. Theophylline levels greater than 16 μg/ml were associated with toxicity (5). For a drug with this narrow therapeutic index, it is difficult to maintain the optimum blood level for the desired time period; higher concentrations frequently result in toxicity and lower values appear less likely to provide maximal therapeutic benefit. Those problems suggest that modification of pharmaceutical properties are necessary to maintain the optimum blood level by the prodrug approach.

One main objective of a prodrug is to influence the plasma drug concentration–time profile with known pharmacological activity. This effect is achieved conveniently when the prodrug is much less soluble in water and has a slower dissolution rate in aqueous fluid than the parent drug. Under these circumstances, the appearance of the parent drug in the body is slowed by the slow dissolution of the prodrug in the GI tract (6–8). The purpose of this study was to investigate some physicochemical properties of 7,7′-succinylditheophylline as a potential prolonged-release theophylline prodrug.

THEORETICAL

The dissolution of 7,7′-succinylditheophylline will be shown to be pH dependent above pH 8. At pH values greater than 8, the hydrolysis of 7,7′-succinylditheophylline to theophylline occurs so rapidly that it takes place in the diffusion layer film. That is, the dissolution of 7,7′-succinylditheophylline occurs with a simultaneous irreversible chemical reaction.

Theoretical predictions of the dissolution rate with simultaneous irreversible chemical reactions have been treated previously (9, 10). The experimental data for the dissolution rate of 7-acetyltheophylline agreed with theoretical predictions based on the film theory model under steady-state conditions. This theoretical treatment also may be applied to 7,7′-succinylditheophylline.

The problem to be considered is that in which a solid phase, A, dissolves into the liquid phase and then reacts irreversibly with a species, B, already present in the liquid phase: $A + B \rightarrow C + D$. The intermediate species, D, then reacts irreversibly with B to form the final products: $D + (n-1)B \rightarrow$ products, where n is the number of molecules of B. If A is 7,7′-succinylditheophylline and B is hydroxide ion, n is equal to 2 below pH 8 and to 4 above pH 9. The first step, disappearance of A by reaction with B, would be considered a rate-determining step.

Let A be the concentration of 7,7′-succinylditheophylline at a distance X within the liquid film, t the time, k_0 the first-order rate constant of a

0022-3549/79/0300-0288$01.00/0

spontaneous hydrolysis reaction, k_B the second-order rate constant for the reaction between solute A and component B, D_A the diffusion coefficient of A in the medium, and D_B the diffusion coefficient of B in the medium.

If the chemical reaction is fast enough, it takes place in a thin zone within the diffusional film; the concentration distribution that establishes the diffusional film is sketched in Fig. 1. The diffusion rate in an element of unit area can be expressed by:

$$W_A = -D_A \frac{dA}{dX} \qquad \text{(Eq. 1)}$$

The diffusion rate out of the element at the point $X + dX$ will be:

$$W'_A = -D_A \left(\frac{dA}{dX} + \frac{d^2A}{dX^2} dX\right) \qquad \text{(Eq. 2)}$$

The consumption rate of A within the element is, therefore:

$$W_A - W'_A = D_A \frac{d^2A}{dX^2} dX \qquad \text{(Eq. 3)}$$

For component B, the analogous expression is:

$$-(W'_B - W_B) = D_B \frac{d^2B}{dX^2} dX \qquad \text{(Eq. 4)}$$

Per unit time, the consumption of A and B is expressed also by the reaction rate:

$$-\frac{dA}{dt} = -\frac{1}{n}\frac{dB}{dt} = (k_0 + k_B B)A \qquad \text{(Eq. 5a)}$$

So that the number of molecules A and B disappearing within the volume element will be:

$$-\frac{dA}{dt} dX = -\frac{1}{n}\frac{dB}{dt} dX = (k_0 + k_B B)A\, dX \qquad \text{(Eq. 5b)}$$

Combining Eqs. 3, 4, and 5b yields:

$$D_A \frac{d^2A}{dX^2} = \frac{D_B}{n}\frac{d^2B}{dX^2} = (k_0 + k_B B)A \qquad \text{(Eq. 6)}$$

A general solution of this equation by exact mathematical methods is not possible. However, one important conclusion can immediately be drawn from the equation since:

$$D_A \frac{d^2A}{dX^2} - \frac{D_B}{n}\frac{d^2B}{dX^2} = 0 \qquad \text{(Eq. 7)}$$

After two integrations, the constants of integration are evaluated to give Eq. 8 by use of boundary conditions:

$$-D_A \left(\frac{dA}{dX}\right)_{x=0} = \frac{D_A}{X_L}(A_0 - A_L) + \frac{D_B}{nXL}(B_L - B_0) \qquad \text{(Eq. 8)}$$

where $X = 0$, $A = A_0$, and $B = B_0$ at the interface and $X = X_L$, $A = A_L$, and $B = B_L$ at the film edge.

Although Eq. 8 represents the dissolution rate of A per unit area of film, it cannot be determined directly from this relationship since the B_0 concentration is unknown. However, it is possible to find a solution for B_0 in specific cases by a numerical integration of Eq. 6.

A mathematical solution of Eq. 6 was described previously (11, 12) for some special cases when the concentration of B (or liquid phase reactants) is constant throughout the liquid film:

$$D_A \left(\frac{d^2A}{dX^2}\right) = (k_0 + k_B B_L)A \qquad \text{(Eq. 9a)}$$

The solution of the equation is given by:

$$A = \frac{A_L \sinh(aX) + A_0 \sinh[a(X_L - X)]}{\sinh(aX_L)} \qquad \text{(Eq. 9b)}$$

where:

$$a = \sqrt{\frac{k_0 + k_B B_L}{D_A}} \qquad \text{(Eq. 9c)}$$

The slope of the concentration curve is obtained by differentiating Eq. 9b. The diffusion rate of A into the solution phase, N_A, is obtained by multiplying the slope at $X = 0$ by the diffusivity, D_A:

$$N_A = -D_A \left(\frac{dA}{dX}\right)_{x=0} = \frac{D_A a\,[A_0 \cosh(aX_L) - A_L]}{\sinh(aX_L)} \qquad \text{(Eq. 10)}$$

and:

$$N_A = \frac{D_A}{X_L}\left(A_0 \frac{Y}{\tanh Y} - A_L \frac{Y}{\sinh Y}\right) \qquad \text{(Eq. 11)}$$

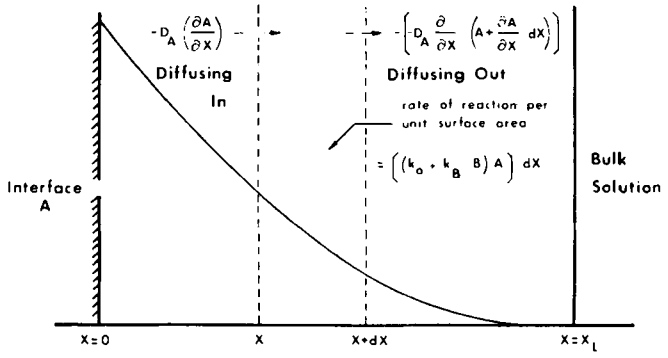

Figure 1—*Schematic illustration of concentration profiles during the dissolution of solid* A *in reactive media. Key:* X, *distance from* A; *and* L, *diffusion layer thickness.*

where $Y = aX_L$.

Consider the following conditions:

1. When the reaction rate is practically zero, Y is nearly equal to sinh Y and tanh Y. Equation 11 is reduced to:

$$N_A = \frac{D_A}{X_L}(A_0 - A_L) \qquad \text{(Eq. 12a)}$$

For the special case where $A_L = 0$:

$$N_A = M_1 = \frac{D_A}{X_L} A_0 \qquad \text{(Eq. 12b)}$$

this value must be considered as the limiting rate of diffusion; *i.e.*, when the reaction proceeds entirely within the bulk of the liquid, diffusion through the liquid film is the rate-determining step.

2. When the reaction rate is large, tanh $Y = 1$ and sinh Y tends toward infinity so Eq. 11 reduces to:

$$N_A = \left(\frac{D_A}{X_L} A_0\right) Y = A_0 \sqrt{(k_0 + k_B B_L) D_A} \qquad \text{(Eq. 13)}$$

At a high reaction rate, the reaction proceeds completely within the liquid film and the overall appearance rate of product (theophylline), R_1, is:

$$R_1 = A_0 \sqrt{(k_0 + k_B B_L) D_A} \qquad \text{(Eq. 14)}$$

EXPERIMENTAL

Measurement of Hydrolysis Rates—Reactions were performed in the cell of a UV spectrophotometer[1]. Appropriate portions (0.5 and 2.5 ml) of 4×10^{-4} *M* 7,7′-succinylditheophylline in dioxane were placed in a 2-cm cell, and buffer solutions (5 and 3 ml) were injected from a syringe into the cell at 25° at the same time as the chart motor was started.

Measurements of the absorbance change at 300 nm were taken. The apparent first-order rate constants were obtained by plotting the net absorbance change against time on semilogarithmic paper and calculating the first-order constant from the equation $k_{app} = 0.693/t_{0.5}$.

Dissolution Rate Determination—Pellets of 7,7′-succinylditheophylline were prepared by directly compressing 200 mg of the material in a die (1.3 cm i.d.) under a force of 454 kg with a laboratory press[2]. The pellet was held firmly in the die by covering the inside surface with melted paraffin (exposed surface area of 1.130 cm^2).

A 500-ml volume of the selected buffer solution was placed in 1-liter, three-necked, round-bottom flasks and kept at 25° in a constant-temperature water bath. A semicircular stirring blade (width of 4.8 cm and maximum depth of 1.4 cm) was positioned in the dissolution medium so that the top of the blade was maintained at the same level as the dissolution medium surface.

The pellet was placed in the medium by guiding it through the side neck of the flask, and it remained at the bottom of the flask without moving during agitation. A stirring rate of 50 rpm was initiated immediately after the pellet was introduced into the flask. At the same time, a sample of the solution was circulated continuously, at a flow rate of 43 ml/min, with a peristaltic pump[3] to a UV spectrophotometer. Absorbances were recorded at 270 nm using a 1-cm flowcell.

[1] Model 14, Cary, Monrovia, CA 91016.
[2] Model C, Fred S. Carver, Menomonee Falls, WI 53051.
[3] Model 7016, Cole-Palmer, Chicago, IL 60648.

Table I—Apparent First-Order Rate Constants (k_{app}, seconds^{-1}) for Hydrolysis of 7,7-Succinylditheophylline in Various Buffer Concentrations and pH Values

Buffer[a]			pH[b]	$k_{app}^{45.5\%}$[c], sec^{-1}	$k_{app}^{9\%}$[d], sec^{-1}
	0.1 N HCl		1.10	3.01×10^{-2}	8.04×10^{-2}
	1×10^{-2} N HCl		2.05	2.95×10^{-2}	
	1×10^{-3} N HCl		3.07	2.95×10^{-2}	8.15×10^{-2}
$[CH_3COOH]$	$[CH_3COONa]$	[NaCl]			
6.0×10^{-4}	1.4×10^{-3}	9.86×10^{-2}	5.05 ± 0.03	2.95×10^{-2}	
1.2×10^{-3}	2.8×10^{-3}	9.72×10^{-2}	5.05 ± 0.03	2.95×10^{-2}	
2.4×10^{-3}	5.6×10^{-3}	9.44×10^{-2}	5.05 ± 0.03	3.01×10^{-2}	
3.6×10^{-3}	8.4×10^{-3}	9.16×10^{-2}	5.05 ± 0.03	2.95×10^{-2}	
			5.05 ± 0.03	2.95×10^{-2} [e]	8.15×10^{-2} [e]
$[Na_2HPO_4]$	$[NaH_2PO_4]$	[NaCl]			
1.4×10^{-3}	1.0×10^{-2}	8.58×10^{-2}	6.0 ± 0.01	3.01×10^{-2}	8.66×10^{-2}
2.8×10^{-3}	2.0×10^{-2}	7.16×10^{-2}	6.0 ± 0.01	3.38×10^{-2}	9.00×10^{-2}
4.2×10^{-3}	3.0×10^{-2}	5.74×10^{-2}	6.0 ± 0.01	3.55×10^{-2}	9.24×10^{-2}
5.7×10^{-3}	4.0×10^{-2}	4.28×10^{-2}	6.0 ± 0.01	3.85×10^{-2}	9.50×10^{-2}
7.0×10^{-3}	5.0×10^{-2}	2.80×10^{-2}	6.0 ± 0.01	4.08×10^{-2}	
			6.0 ± 0.01	2.79×10^{-2} [e]	8.34×10^{-2} [e]
4.88×10^{-3}	3.12×10^{-3}	8.22×10^{-2}	6.95 ± 0.05	4.47×10^{-2}	9.90×10^{-2}
7.32×10^{-3}	4.68×10^{-3}	7.34×10^{-2}	6.95 ± 0.05	4.62×10^{-2}	10.27×10^{-2}
9.76×10^{-3}	6.24×10^{-3}	6.45×10^{-2}	6.95 ± 0.05	5.33×10^{-2}	10.66×10^{-2}
12.20×10^{-3}	7.80×10^{-3}	5.56×10^{-2}	6.95 ± 0.05	5.54×10^{-2}	11.19×10^{-2}
			6.95 ± 0.05	3.62×10^{-2} [e]	9.02×10^{-2} [e]
1.0×10^{-2}	2.34×10^{-3}	1.68×10^{-1}	7.40 ± 0.05	7.70×10^{-2}	
2.0×10^{-2}	4.70×10^{-3}	1.35×10^{-1}	7.40 ± 0.05	8.35×10^{-2}	
4.0×10^{-2}	9.38×10^{-3}	9.06×10^{-2}	7.40 ± 0.05	9.90×10^{-2}	
5.0×10^{-2}	11.72×10^{-3}	3.83×10^{-2}	7.40 ± 0.05	10.83×10^{-2}	
			7.40 ± 0.05	6.85×10^{-2} [e]	
1.88×10^{-2}	3.12×10^{-2}	11.20×10^{-2}	6.46	4.62×10^{-2}	
2.45×10^{-2}	2.55×10^{-2}	10.10×10^{-2}	6.07	4.78×10^{-2}	
3.05×10^{-2}	1.95×10^{-2}	8.90×10^{-2}	6.89	6.93×10^{-2}	
3.60×10^{-2}	1.40×10^{-2}	7.80×10^{-2}	7.12	7.70×10^{-2}	
4.05×10^{-2}	9.50×10^{-3}	6.90×10^{-2}	7.35	9.90×10^{-2}	
4.35×10^{-2}	6.50×10^{-3}	6.30×10^{-2}	7.54	10.66×10^{-2}	
4.58×10^{-2}	4.20×10^{-3}	5.81×10^{-2}	7.74	14.66×10^{-2}	

[a] Values in the aqueous medium without dioxane. [b] All pH values were measured in aqueous buffers at 25° before mixing with dioxane. [c] The apparent first-order rate constant (seconds^{-1}) for the reaction in 45.5% dioxane–54.5% aqueous buffer solution. [d] The apparent first-order rate constant (seconds^{-1}) for the reaction in 9% dioxane–91% aqueous buffer solution. [e] Values obtained by extrapolation to zero buffer concentration.

The total amount of compound in solution as a function of time was determined. The total dissolution rate of 7,7′-succinylditheophylline, $(dA/dt)_{t=0}$, was obtained from the initial slope of the concentration–time curve, and the dissolution rate per unit area of the pellet was obtained from the value of $(V/S)(dA/dt)_{t=0}$, where V is the dissolution medium volume of 500 ml and S is the pellet surface area of 1.13 cm^2. 7,7′-Succinylditheophylline was measured in solution as theophylline since, as will be shown later, 7,7′-succinylditheophylline rapidly and quantitatively reverted to theophylline at all pH values studied.

RESULTS AND DISCUSSION

Spectral Change and Molar Absorptivity—The spectra of 7,7′-succinylditheophylline showed a λ_{max} at 300 nm in dioxane (Fig. 2, curve 1). After 3 ml of 1×10^{-4} M 7,7′-succinylditheophylline in dioxane was mixed with 0.5 ml of water, the spectra were taken at appropriate time intervals (4–10 min, Fig. 2, curves 2–6); the initial absorbance at 300 nm in dioxane (λ_{max} of 7,7′-succinylditheophylline) decreased with time. A new band appeared at 274 nm (λ_{max} of theophylline). The λ_{max} at 300 nm completely disappeared within 1.5 hr (Fig. 2, curve 7). Maintenance of an apparent isosbestic point at 287 nm was evident for the transformation of 7,7′-succinylditheophylline.

Appropriate volumes of 7,7′-succinylditheophylline stock solution (1×10^{-4} M) in dioxane were diluted with 0.1 N HCl to give a 4×10^{-5}–1×10^{-5} M range, and spectra were taken with a 5-cm silica cell after overnight standing at room temperature. Molar absorptivities of degraded 7,7′-succinylditheophylline and theophylline at 270 nm were 2.025×10^4 and 1.003×10^4 liters/mole-cm, respectively. These data showed that molar absorptivity of degraded 7,7′-succinylditheophylline in 0.1 N HCl was two times greater than that of theophylline. This information, coupled with the spectral change (from 300 to 270 nm), demonstrated that 1 mole of 7,7′-succinylditheophylline degraded to produce 2 moles of theophylline.

Catalytic Hydrolysis Rate Constants—No significant buffer catalysis was observed in the acetate buffer and dioxane mixture with an ionic strength of 0.1 (Table I). However, a small, but significant, buffer effect was observed with phosphate buffer. The apparent first-order rate constant at zero phosphate buffer concentration was obtained from plots of the apparent first-order rate constants, k_{app}, against the phosphate buffer concentration (Table I and Fig. 3).

No specific acid catalysis was observed (Fig. 4). The important contribution to hydrolysis of 7,7′-succinylditheophylline at the pH-independent region below pH 6 would be water catalysis. The apparent first-order rate constant for a 9% dioxane–91% aqueous system below pH 6 was $k_{app}^{9\%} = 8.15 \times 10^{-2}$ sec (Table I and Fig. 4). The extrapolated value, k_0, agreed reasonably with the $k_0^{9\%}$ value. It was based on the premise that the results in a 9% dioxane–water system are very similar to those in pure water systems (13). Above pH 7, the hydrolysis kinetics in a 9% dioxane–buffer system were difficult to follow by conventional UV spectrophotometry because of the rapid hydrolytic reaction.

The specific base catalytic constant, $k_{OH^-}^{45.5\%}$, in a 45.5% dioxane–55.5% aqueous buffer system was obtained from plots of k_{app} against $[OH^-]$ (where pH was measured in pure aqueous buffer with ionic strength 0.2); $k_{OH^-}^{45.5\%}$ was 1.46×10^5 liters/mole-sec (Fig. 5). Because the value of $k_{OH^-}^{45.5\%}$ was obtained from the apparent hydroxide-ion concentration, ranging from 10^{-6} to 10^{-8} M, the activity coefficient of OH^- in a 45.5% dioxane–water system, $\gamma_{OH^-}^{45.5\%}$, as well as the activity coefficient of OH^- in water, $\gamma_{OH^-}^{0\%}$, can be assumed to be unity, so the value of $k_{OH^-}^{45.5\%}$ can be treated as that of the specific base catalytic constant in water, k_{OH^-}.

Based on those values of k_0 and k_{OH^-}, the theoretical log k_{app}–pH profiles were constructed as shown in Fig. 4.

Hydrolytic Reactivity and Mechanisms—7-Acetyltheophylline (I) and 7,7′-succinylditheophylline have half-lives of 40 and 8 sec, respec-

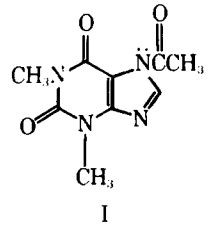

I

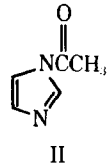

II

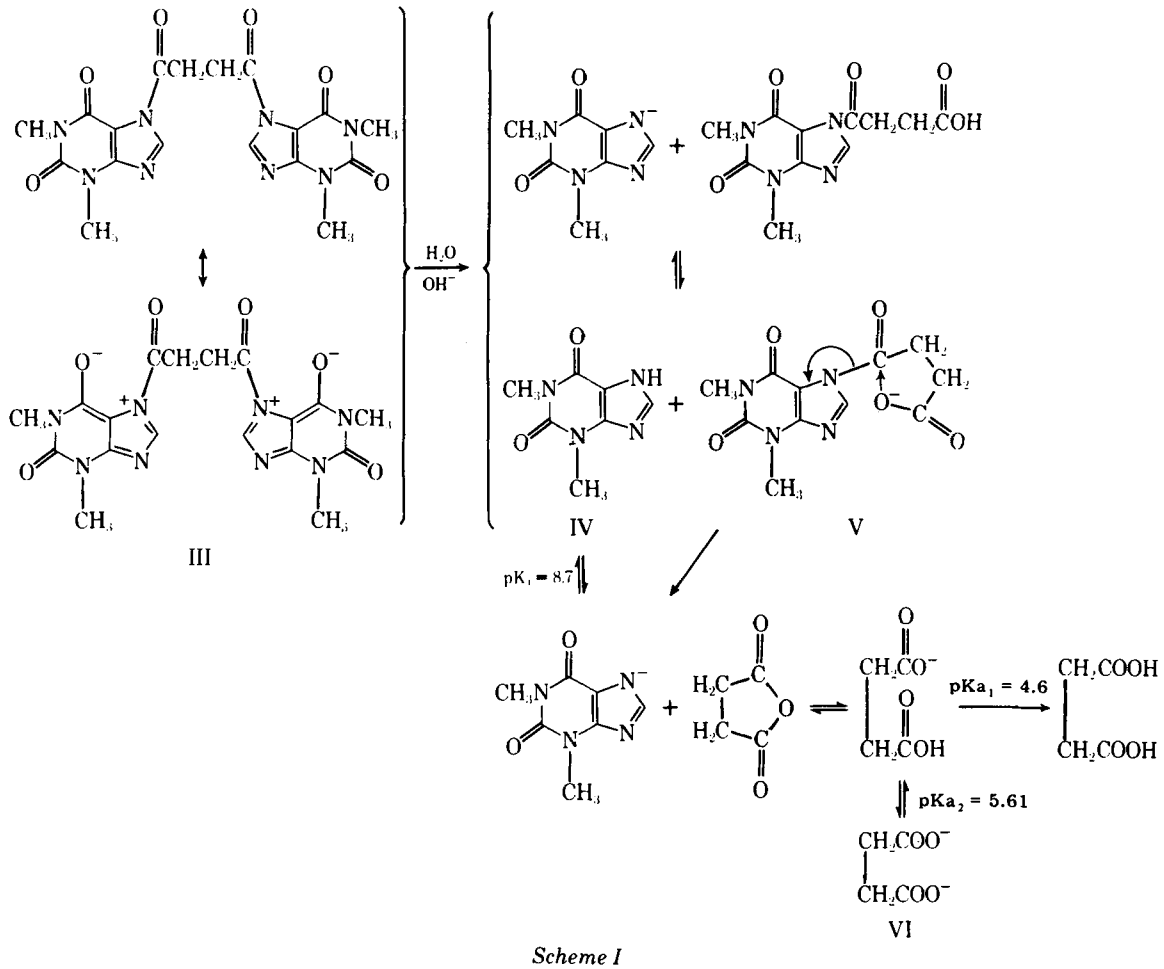

Scheme I

tively, in water at room temperature. The high degree of reactivity of *N*-acylated theophylline compounds compared with the low reactivity of normal amides may be related to the quasiaromatic character of the theophylline ring. As a result of the participation of the electron pair on the 7-nitrogen in the π-electron system, this nitrogen becomes more positive, exerting attraction toward the ring. This electron attraction increases the rate of nucleophilic reactions involving the carbonyl group.

N-Acetylimidazole (II) is hydrolyzed with a half-life of 40 min at room temperature in water (14). The difference in reactivity between *N*-acylated theophylline compounds and *N*-acetylimidazole can be explained by the greater delocalization of the lone electron pair of the imide nitrogen in the theophylline ring (I) than in the imidazole ring (II). Higher reactivity of 7,7′-succinylditheophylline over 7-acetyltheophylline was expected since the theophylline hemisuccinate group is much better as a leaving group than is the acetyl group.

The overall hydrolytic degradation of 7,7′-succinylditheophylline is illustrated in Scheme I. It is assumed that 7,7′-succinylditheophylline (III) hydrolyzes to theophylline (IV) and theophylline hemisuccinate (V); then the latter degrades to theophylline and the succinate ion (VI) as a consecutive first-order process as shown in Scheme II:

$$A \xrightarrow{k_1} C + D$$

$$D \xrightarrow{k_2} C + E$$

Scheme II

In this study, the kinetics were followed by the disappearance of 7,7′-succinylditheophylline under pseudo-first-order conditions. Experimentally, k_1 and k_2 were inseparable, given by a single exponential decrease in starting material as a function of time. The intermediate, V, could not be isolated by the chromatographic method. It suggested that k_2 is much larger than k_1, so the first step is rate determining.

The hydrolysis of hemisuccinate is catalyzed powerfully by a suitably spaced, neighboring ionized carboxyl group (15, 16). The intramolecular hydrolysis rate of phenyl succinate (VII) at 25° is 1.42×10^{-3} sec^{-1} at neutral pH (16). However, the intermolecular reaction rate of phenyl acetate (VIII) with acetate ion at 63° is 1.02×10^{-5} liter/mole-sec (14).

The intermolecular reaction of phenyl acetate with acetate ion requires more than 100 *M* acetate ion for the hydrolysis rate to be equivalent to the rate of the intramolecular hydrolysis of phenyl succinate. Furthermore, under favorable conditions, the effect of the carboxylate attack is much larger than the effect of hydrogen- and hydroxide-ion-catalyzed ester hydrolysis (16). Therefore, the hydrolysis rate of 7,7′-succinylditheophylline can be expected to be no less than 100-fold of that of 7-acetyltheophylline (1.6×10^{-2} sec), so $k_2 \gg k_1$ (first step is rate determining).

Estimation of Diffusion Coefficient—The values of the diffusion coefficient for 7,7′-succinylditheophylline and hydroxide ion were estimated using the Stokes–Einstein equation (17):

$$D = \frac{RT}{6\pi\mu N}\sqrt[3]{\frac{4\pi N}{3M\nu}} \qquad \text{(Eq. 15)}$$

where M is the molecular weight, ν is the partial specific volume, T is the absolute temperature, R is the molar gas constant, N is Avogadro's number, and μ is the solvent viscosity.

When $\nu = 1$ and $\mu = 0.01$ poise, the values of the diffusion coefficient of 7,7′-succinylditheophylline, D_A, and hydroxide ion, D_B, at 25° were 3.90×10^{-6} and 1.15×10^{-5} cm^2/sec, respectively.

Estimations of Film Thickness, X_L, and Saturation Solubility, A_0—The dissolution rate of A per unit area of film is represented by Eq. 8. The value of A_L is assumed to be zero under the steady-state condition,

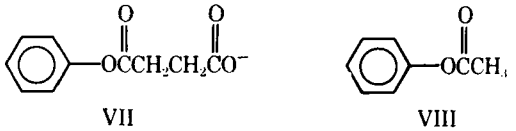

Table II—Comparison of Reaction Time (t_r) and Diffusion Time[a] (t_D = 2 sec) with Respect to Various pH Values

pH	[OH⁻], mole/cm³	k_{app}[b], sec⁻¹	t_r[c], sec
1.0	1×10^{-16}	8.15×10^{-2}	12.27
3.0	1×10^{-14}	8.15×10^{-2}	12.27
5.0	1×10^{-12}	8.16×10^{-2}	12.25
7.0	1×10^{-10}	9.61×10^{-2}	10.41
9.0	1×10^{-8}	1.54	6.49×10^{-1}
10.14	1.38×10^{-7}	2.02×10^{1}	4.94×10^{-2}
11.0	1.0×10^{-6}	1.46×10^{2}	6.85×10^{-3}
11.7	5.0×10^{-6}	7.30×10^{2}	1.37×10^{-3}
12.0	1.0×10^{-5}	1.46×10^{3}	6.85×10^{-4}
12.48	3.0×10^{-5}	4.38×10^{3}	2.28×10^{-4}
12.70	5.0×10^{-5}	7.30×10^{3}	1.37×10^{-4}
13.0	1.0×10^{-4}	1.46×10^{4}	6.85×10^{-5}
13.3	2.0×10^{-4}	2.92×10^{4}	3.42×10^{-5}
13.48	3.0×10^{-4}	4.38×10^{4}	2.28×10^{-5}

[a] $t_D = (X_L^2)/(2D_A)$, where $X_L = 3.87 \times 10^{-3}$ cm and $D_A = 3.90 \times 10^{-6}$ cm²/sec. [b] $k_{app} = k_0 + k_{OH^-}[OH^-]$, where $k_0 = 8.15 \times 10^{-2}$ sec⁻¹ and $k_{OH^-} = 1.46 \times 10^8$ cm³/mole-sec. [c] $t_r = 1/k_{app}$.

and rearrangement of Eq. 8 gives:

$$D_A\left(\frac{dA}{dX}\right)_{x=0} = \left(\frac{D_A}{X_L}A_0 - \frac{D_B}{nB_L}B_0\right) + \frac{D_B}{nX_L}B_L \qquad \text{(Eq. 16)}$$

When the chemical reaction takes place mainly in the film, film thickness X_L can be obtained from the slope of the plot of $D_A(dA/dX)_{x=0}$, which is equal to $(V/S)(dc/dt)_{t=0}$, against $[OH^-]$ (Fig. 6). The value of X_L obtained from this plot is 3.87×10^{-3} cm.

The value of X_L also can be obtained under the same hydrodynamic conditions as those for theophylline. With the values of the total dissolution rate of theophylline (1.43×10^{-10} mole/cm³-sec), the saturation solubility (4×10^{-5} mole/cm³), and the diffusion coefficient of theophylline estimated from the Stokes-Einstein equation (5.26×10^{-6} cm²-sec), the value of X_L, 3.33×10^{-3} cm, was obtained from the Noyes-Nernst equation in an analogous manner to previous work (9). Those two estimated values of X_L agreed reasonably well with each other within experimental error.

Direct measurement of the solubility of 7,7′-succinylditheophylline (III) was impossible because of its high reactivity in water ($t_{0.5}$ = 8.0 sec below pH 6). However, with the values of the initial dissolution rate at the pH-independent region, $(V/S)(dc/dt)_{t=0} = 1.78 \times 10^{-9}$ mole/cm²-sec, k_{app} below pH 6 (8.15×10^{-2} sec), D_A, and X_L, the saturation solubility can be estimated from Eqs. 11 and 13, assuming that A_L is equal to zero, so that:

$$A_0 = \frac{X_L}{D_A}\left(\frac{\tanh Y}{Y}\right)N_A \qquad \text{(Eq. 17a)}$$

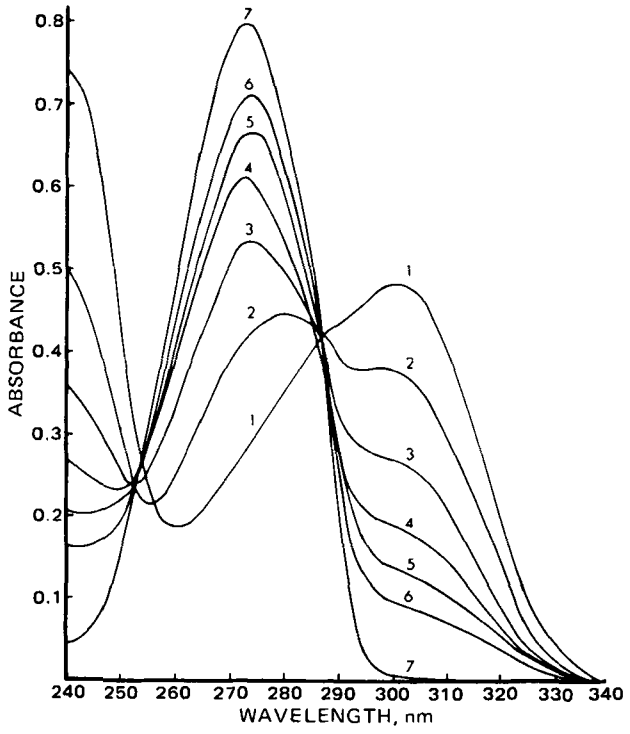

Figure 2—*UV spectral changes for the hydrolysis of 7,7′-succinylditheophylline (1×10^{-4} M) in an 85.7% dioxane and 14.3% water system at 25°.*

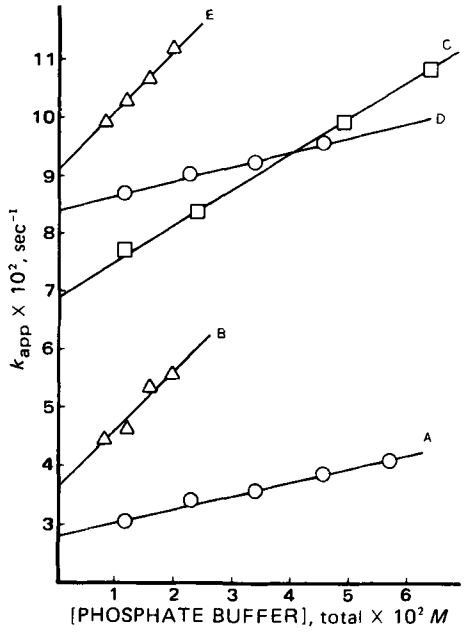

Figure 3—*Plots of apparent first-order rate constants (k_{app}) against various concentrations of phosphate buffer at a constant pH and an ionic strength of 0.1. Curves I, II, and III show the reactions in a 45.5% dioxane-54.5% aqueous buffer system at pH 6.0, 7.0, and 7.4, respectively. Intercept values were: I, 2.79×10^{-2} sec; II, 2.62×10^{-2} sec⁻¹; and III, 6.85×10^{-2} sec⁻¹. Curves IV and V show the reactions in a 9% dioxane-91% aqueous buffer system at pH 6.0 and 7.0, respectively. Their intercept values were: IV, 8.34×10^{-2} sec⁻¹; and V, 9.20×10^{-2} sec⁻¹.*

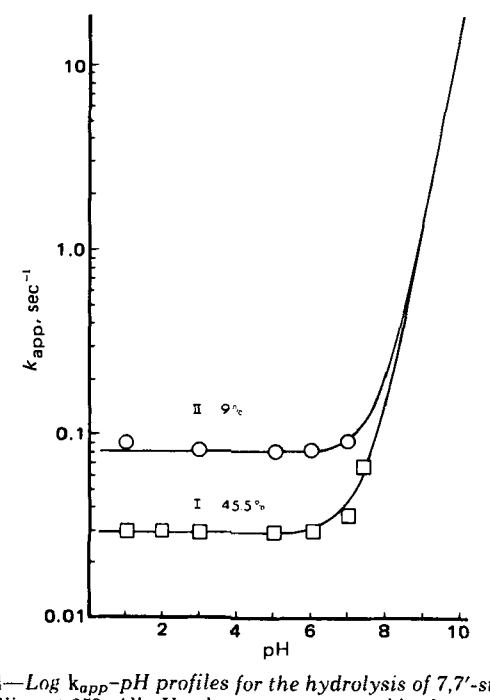

Figure 4—*Log k_{app}-pH profiles for the hydrolysis of 7,7′-succinylditheophylline at 25°. All pH values were measured in the pure aqueous system before the reaction started. Curves I and II show the reactions in 45.5 and 9% dioxane systems, respectively.*

Table III—Dissolution Rates, $(V/S)(dL/dt)_{t=0}$, as a Function of the Buffer Concentration at Various pH Values

Buffer			pH[a]	$V/S(dL/dt)_{t=0}$, mole/cm²-sec
	0.1 *N* HCl		1.0	1.78×10^{-9}
[HCOOH]	[NaOH]	[Buffer]total		
0.05	0.01	0.06	3.1	1.90×10^{-9}
CH_3COOH	$[CH_3COONa]$	[Buffer]total		
1.12×10^{-2}	4.80×10^{-3}	1.60×10^{-2}	5.0 ± 0.05	1.98×10^{-9}
2.24×10^{-2}	9.60×10^{-3}	3.20×10^{-2}	5.0 ± 0.05	1.82×10^{-9}
3.36×10^{-2}	14.40×10^{-3}	4.80×10^{-2}	5.0 ± 0.05	1.75×10^{-9}
6.40×10^{-2}	19.20×10^{-3}	6.40×10^{-2}	5.0 ± 0.05	1.95×10^{-9}
			5.0 ± 0.05	1.88×10^{-9} [b]
$[KH_2PO_4]$	[NaOH]	[Buffer]total		
3.0×10^{-2}	1.78×10^{-2}	4.78×10^{-2}	7.0 ± 0.07	2.09×10^{-9}
4.0×10^{-2}	2.37×10^{-2}	6.37×10^{-2}	7.0 ± 0.07	2.21×10^{-9}
5.0×10^{-2}	2.96×10^{-2}	7.95×10^{-2}	7.0 ± 0.07	2.26×10^{-9}
6.0×10^{-2}	3.55×10^{-2}	9.55×10^{-2}	7.0 ± 0.07	2.27×10^{-9}
			7.0 ± 0.07	1.78×10^{-9} [c]
[Glycine]	[NaOH]	[Buffer]total		
2.0×10^{-2}	3.52×10^{-3}	2.35×10^{-2}	9.0 ± 0.05	3.05×10^{-9}
3.0×10^{-2}	5.29×10^{-3}	3.53×10^{-2}	9.0 ± 0.05	3.50×10^{-9}
3.0×10^{-2}	5.29×10^{-3}	3.53×10^{-2}	9.0 ± 0.05	3.50×10^{-9}
4.0×10^{-2}	7.04×10^{-3}	4.70×10^{-2}	9.0 ± 0.05	3.93×10^{-9}
5.0×10^{-2}	8.80×10^{-3}	5.88×10^{-2}	9.0 ± 0.05	4.39×10^{-9}
6.0×10^{-2}	10.55×10^{-3}	7.06×10^{-2}	9.0 ± 0.05	4.83×10^{-9}
			9.0 ± 0.05	2.18×10^{-9} [c]
$[K_2CO_3]$	$[KHCO_3]$	[Buffer]total		
1.2×10^{-2}	0.8×10^{-2}	2.0×10^{-2}	10.14 ± 0.01	5.03×10^{-9}
2.4×10^{-2}	1.6×10^{-2}	4.0×10^{-2}	10.14 ± 0.01	7.79×10^{-9}
3.6×10^{-2}	2.4×10^{-2}	6.0×10^{-2}	10.14 ± 0.01	9.51×10^{-9}
4.8×10^{-2}	3.2×10^{-2}	8.0×10^{-2}	10.14 ± 0.01	12.24×10^{-9}
6.0×10^{-2}	4.0×10^{-2}	10.0×10^{-2}	10.14 ± 0.01	14.50×10^{-9}
			10.14 ± 0.01	2.77×10^{-9} [c]
	1×10^{-3} *N* NaOH		11.0	3.42×10^{-9}
	5×10^{-3} *N* NaOH		11.7	5.69×10^{-9}
	1×10^{-2} *N* NaOH		12.0	9.21×10^{-9}
	3×10^{-2} *N* NaOH		12.5	2.55×10^{-8}
	5×10^{-2} *N* NaOH		12.7	4.24×10^{-8}
	0.1 *N* NaOH		13.0	7.08×10^{-8}
	0.2 *N* NaOH		13.3	1.45×10^{-7}
	0.3 *N* NaOH		13.5	2.30×10^{-7}

[a] The pH values in hydrochloric acid and sodium hydroxide were calculated under the assumption that activity coefficient of hydrochloric acid and sodium hydroxide was unity. [b] Average value at constant pH. [c] Values obtained by extrapolation to zero buffer concentration.

where:

$$Y = X_L \sqrt{\frac{k_{app}}{D_A}} \qquad \text{(Eq. 17b)}$$

and:

$$A_0 = \frac{X_L}{D_A} \frac{V}{S} \left(\frac{dA}{dt}\right)_{t=0} \qquad \text{(Eq. 17c)}$$

where:

$$\frac{V}{S}\left(\frac{dA}{dt}\right)_{t=0} = D_A \left(\frac{dA}{dt}\right)_{t=0} \qquad \text{(Eq. 17d)}$$

The value of A_0 at 25° was found to be 1.61×10^{-6} mole/cm³ from Eq. 17a and 1.67×10^{-6} mole/cm³ from Eq. 17c.

Another way of estimating solubility is from the intercept value, $(D_A/X_L)A_0 - (D_B/nX_L)B_0 = 1.242 \times 10^{-9}$ mole/cm², of the plots of $D_A (dA/dX)_{x=0}$ *versus* $[OH^-]$ (Fig. 6). With the assumption that B_0 was equal to zero, A_0 was estimated to be 1.21×10^{-6} mole/cm³ from Eq. 17c, and best fit the experimental values according to:

$$R = \frac{D_A}{X_L} A_0 + \frac{D_B}{nX_L} B_L \qquad \text{(Eq. 18)}$$

Estimations of Diffusion Time and Reaction Time—The diffusion time, t_D, for steady state was derived previously (8, 9):

$$t_D = \frac{X_L^2}{2D_A} \qquad \text{(Eq. 19)}$$

The physical meaning of the diffusion time is the average lifetime for element A to travel through distance X_L, and it depends on the hydrodynamic conditions. According to Eq. 19, the estimated value of the diffusion time of III was 2 sec.

A useful concept in the analysis of a chemical reaction is the reaction time, t_r, defined (18) as A/r, where r is the chemical reaction rate and A is the actual initial concentration of the reactant. For a simple first-order reaction with a kinetic constant k_{app}:

$$t_r = \frac{1}{k_{app}} \qquad \text{(Eq. 20)}$$

Thus, at the end of the reaction time, 63% of III will have undergone reaction with first-order kinetics. The reaction times under various pH conditions are shown in Table II. These times are useful in analyzing dissolution kinetics.

Comparison of Estimated and Measured Dissolution Rates—The dissolution rates at various pH values were obtained by extrapolating to zero buffer concentration (Table III and Fig. 7). At pH values below

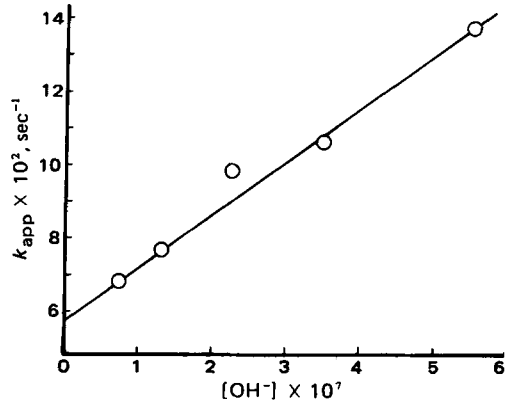

Figure 5—*Plot of apparent first-order rate constants* (k_{app}) *for the hydrolysis of 7,7'-succinylditheophylline in 45.5% dioxane–54.5% aqueous buffer system at pH 6.89–7.74 with a constant phosphate buffer concentration (0.1 M) and an ionic strength of 0.2 at 25°. The value of the slope* ($k_{OH}^{45.5\%}$) *was 1.45 × 10⁻⁵ liter/mole-sec.*

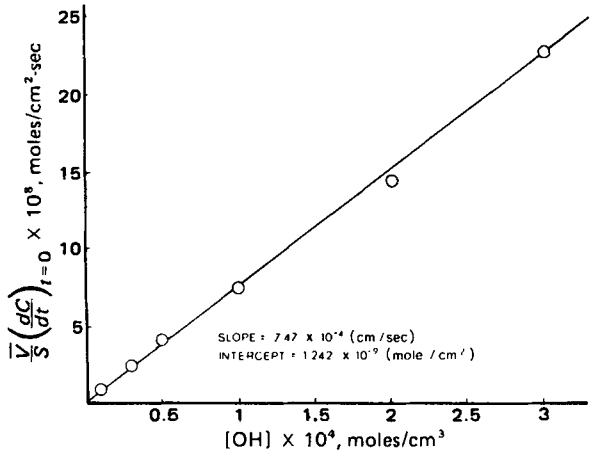

Figure 6—*Plots of the initial dissolution rate,* $(V/S)(dC/dt)_{t=0}$, *against the hydroxide-ion concentration. The slope of the plot* (D_B/nXL) *was* 7.4×10^{-4} *cm/sec.*

7, the reaction times were about sixfold greater than the diffusion time of 2 sec under these experimental conditions. The observed dissolution rate depends on the diffusion time rather than reaction time. The rate-determining factor is the diffusion rate of III from the solid–liquid interface into the bulk of the solution. The theoretical dissolution rates in these cases were estimated from the simplified equations and all led to Eq. 21 when A_L and B_0 were assumed to be zero under the sink conditions, respectively:

$$N_A = \frac{D_A}{X_L} A_0 \left(\frac{Y}{\tanh Y}\right) \qquad \text{(Eq. 21)}$$

Also, in Eq. 18, the second term, $(D_B/nX_L)B_L$, can be neglected in comparison with the first term, $M_1 = (D_A/X_L)A_0$, so that the overall dissolution rate is independent of pH and governed by M_1. The results obtained experimentally agreed fairly well with analytical solutions to Eqs. 18 and 21 (Table IV and Fig. 8).

At pH 9–11, the reaction times, t_r, were small compared to the diffusion time, t_0, of 2 sec. Thus, the chemical reactions were fast enough to proceed in the diffusion layer so that the dissolution rate was affected by $[OH^-]$.

The estimated values from Eq. 18 and the observed values at pH 9, 10, 11, and 14 were reached within experimental error (Table IV and Fig. 8).

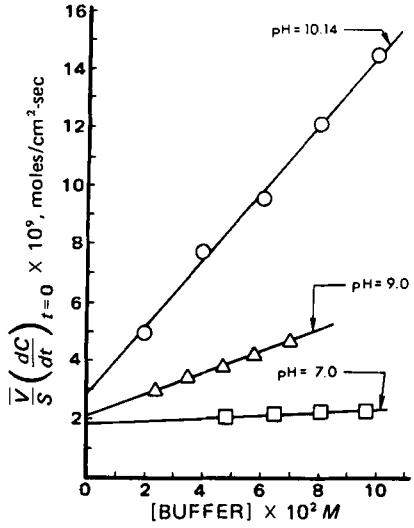

Figure 7—*Plots of the initial dissolution rate,* $(V/S)(dC/dt)_{t=0}$, *against buffer concentrations. The buffer systems were monobasic potassium phosphate–sodium hydroxide (pH 7.0), glycine–sodium hydroxide (pH 9.0), and potassium carbonate–potassium bicarbonate (pH 10.14). The intercepts were* 1.78×10^{-9}, 2.18×10^{-9}, *and* 2.77×10^{-9}, *respectively.*

Table IV—Comparison of Theoretical and Experimental Dissolution Rates at Each pH

pH	$M_2 = (D_B/nX_L)BL$[a], mole/cm²-sec	$R = M_1 + M_2$[b], mole/cm²-sec	$V/S(dC/dt)_{t=0}$[c], mole/cm²-sec
1.0	—	1.78×10^{-9}	1.78×10^{-9}
3.0	—	1.78×10^{-9}	1.78×10^{-9}
5.0	1.49×10^{-15}	1.78×10^{-9}	1.69×10^{-9}
7.0	1.49×10^{-13}	1.78×10^{-9}	1.78×10^{-9}
9.0	7.45×10^{-12}	1.79×10^{-9}	2.18×10^{-9}
10.14	1.03×10^{-10}	1.88×10^{-9}	2.77×10^{-9}
11.0	7.47×10^{-10}	2.53×10^{-9}	3.42×10^{-9}
11.7	3.73×10^{-9}	5.51×10^{-9}	5.69×10^{-9}
12.0	7.46×10^{-9}	9.24×10^{-9}	9.21×10^{-9}
12.48	2.24×10^{-8}	2.42×10^{-8}	2.55×10^{-8}
12.70	3.73×10^{-8}	3.91×10^{-8}	4.24×10^{-8}
13.0	7.46×10^{-8}	7.64×10^{-8}	7.08×10^{-8}
13.3	1.49×10^{-7}	1.51×10^{-7}	1.40×10^{-7}
13.48	2.24×10^{-7}	2.26×10^{-7}	2.30×10^{-7}

[a] Below pH 7, $n = 2$; above pH 9, $n = 4$; $D_B = 1.155 \times 10^{-5}$ cm²/sec; $X_L = 3.87 \times 10^{-3}$ cm. [b] Theoretically estimated values according to Eq. 19, where $M_1 = (DA)/(X_L)A_0 = 1.78 \times 10^{-9}$. [c] Experimentally measured values.

From these data, it is apparent that the dissolution rate is controlled by the diffusion rate of A as well as that of B $[OH^-]$, resulting in curvature of the logarithmic dissolution rate–pH rate profile (Fig. 8).

At pH >11.7, the reactions were sufficiently fast to take place in a diffusion layer, because the reaction times were extremely small (10^{-3}–10^{-5}-fold) compared with the diffusion time of 2 sec (Table II). The observed values of the dissolution rates agreed with the estimated values from Eq. 18. Thus, the rate-controlling phenomenon is the diffusion rate of hydroxide ion from the bulk solution to the solid–liquid interface, and the dissolution rate is greatly increased with a rise in the hydroxide-ion concentration; *i.e.*, the dissolution rate is linearly dependent on the pH in this region (Fig. 8).

Log Dissolution Rate–pH Profile—The log dissolution rate–pH profile (Fig. 8) exhibits a break point at pH 11 between the pH-independent and pH-dependent regions, whereas the log k_{app}–pH profile (Fig. 4) has a break point at pH 7. The ascending slope for the hydrolytic reaction is theoretically unity; however, that observed for the dissolution rate is 0.94 (theoretically estimated value, 0.94). These two differences in the dissolution plot can be rationalized adequately on the basis of a model system.

From the mathematical model, a general solution of Eq. 8 for the dissolution rate was obtained. The dissolution rate increased with a rise in the value of the second term of the equation, $(D_B/nX_L)(B_L - B_0)$, *i.e.*, with the value of B_L. The dissolution rate at the ascending part of the profile (above pH 12) was slightly influenced by the first term of the equation, $(D_A/X_L)(A_0 - A_L)$, where A_L was assumed to be zero under

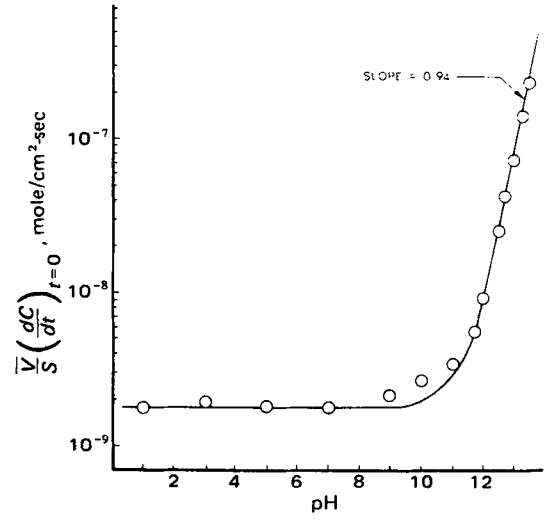

Figure 8—*Plots of the logarithmic dissolution rate against pH at 25°, where the values at pH 7, 9, and 10.14 were obtained by extrapolation to zero buffer concentration and the pH values in sodium hydroxide were calculated under the assumption that the activity coefficient of sodium hydroxide was unity.*

the sink condition (compared with M_1 and M_2 in Table IV). The deviation from the slope of unity existed as long as some degree of the first term, $(D_A/X_L)A_0$, affected the dissolution rate. The break point difference can be explained by the differences between $k_{OH^-}[OH^-] - k_0$ and $(D_B/nX_L)B_L - (D_A/X_L)A_0$.

SUMMARY AND CONCLUSION

The prodrug, 7,7′-succinylditheophylline, was hydrolyzed with a half-life of about 10 sec in the physiological pH range. These hydrolysis studies suggested that the prodrug would hydrolyze very rapidly and release the parent molecule, theophylline, once it was dissolved.

The dissolution rate of 7,7′-succinylditheophylline was 35 times slower than that of theophylline under the same conditions, and its dissolution rate was independent of pH within the physiological pH range. Dissolution rate studies coupled with hydrolysis rate studies suggested that the dissolution process would be the rate-determining step to keep the steady-state release into solution (Scheme III).

$$\text{prodrug in solid} \xrightarrow[\text{slow process}]{\text{dissolution}} \text{prodrug in solution} \xrightarrow[\text{rapid process}]{\text{hydrolysis}} \text{parent drug in solution}$$

Scheme III

The saturation solubility of 7,7′-succinylditheophylline at 25° in water was estimated to be 1.63×10^{-3} M from the rate dissolution data. Under the same conditions, theophylline solubility was 4×10^{-2} M. From these results, it appears that 7,7′-succinylditheophylline might be a valuable candidate as a prolonged-release theophylline prodrug.

REFERENCES

(1) R. Maselli, G. L. Casal, and E. F. Ellis, *J. Pediatr.*, **76**, 777 (1970).

(2) R. H. Jackson, J. I. McHenry, F. B. Moreland, W. J. Raymer, and R. L. Etter, *Dis. Chest*, **45**, 75 (1974).

(3) D. P. Nicholson and T. W. Chick, *Am. Rev. Respir. Dis.*, **108**, 241 (1973).

(4) P. A. Mitenko and R. I. Ogilvie, *N. Engl. J. Med.*, **289**, 600 (1973).

(5) J. W. Jenne, E. Wyze, B. S. Rood, and R. M. MacDonald, *Clin. Pharmacol. Ther.*, **13**, 349 (1972).

(6) R. E. Notari, *J. Pharm. Sci.*, **62**, 865 (1973).

(7) A. A. Sinkula and S. H. Yalkowsky, *ibid.*, **64**, 3259 (1975).

(8) T. Higuchi and V. Stella, "Pro-drugs as Novel Drug Delivery Systems," ACS Symposium Series 14, American Chemical Society, Washington, D.C., 1975.

(9) H. K. Lee, Ph.D. thesis, University of Kansas, Lawrence, Kans., 1970.

(10) T. Higuchi, H. K. Lee, and I. H. Pitman, *Farm. Aikak.*, **80**, 55 (1971).

(11) D. W. Van Krevelen and P. J. Hoftijer, *Rec. Trav. Chim. Pays-Bas*, **67**, 563 (1948).

(12) T. K. Sherwood and R. L. Pigford, "Absorption and Extraction," McGraw-Hill, New York, N.Y., 1952, p. 327.

(13) H. S. Harnetand and B. B. Owen, "The Physical Chemistry of Electrolytic Solutions," 3rd ed., Reinhold, New York, N.Y., 1958, p. 453.

(14) T. C. Bruice and S. J. Benkovic, "Bioorganic Mechanisms," vol. I, Benjamin, New York, N.Y., 1966, p. 61.

(15) M. L. Bender, F. Chloupek, and M. C. Neven, *J. Am. Chem. Soc.*, **80**, 5384 (1958).

(16) E. Gaetigens and H. Morawetz, *ibid.*, **82**, 5328 (1960).

(17) A. N. Martin, J. Swarbrick, and A. Cammarata, "Physical Pharmacy," 2nd ed., Lea & Febiger, Philadelphia, Pa., 1969, p. 452.

(18) G. Astarita, "Mass Transfer with Chemical Reaction," Elsevier, New York, N.Y., 1967, p. 9.

ACKNOWLEDGMENTS

Supported jointly by G. D. Searle and Co. and INTERx Research Corp. Some of the work at the University of Kansas was supported by National Institutes of Health Grant GM 22357.

The authors deeply appreciate the cooperation of Dr. N. Bodor, Dr. K. B. Slaon, and Dr. Y. N. Kuo of INTERx Research Corp. and Mr. C. Kim of G. D. Searle & Co. for providing the 7,7′-succinylditheophylline. Thanks are also extended to Dr. Y. W. Chien, Searle Laboratories, for reviewing this manuscript.

Beneficial Effects of Methionine and Histidine in Aspirin Solutions on Gastric Mucosal Damage in Rats

JAMES K. LIM ˣ, PREM K. NARANG *, DENNIS O. OVERMAN, and ARTHUR I. JACKNOWITZ

Received March 10, 1978, from the *School of Pharmacy and Department of Anatomy, Medical Center, West Virginia University, Morgantown, WV 26506.* Accepted for publication August 3, 1978. *Present address: School of Pharmacy, University of Maryland, Baltimore, MD 21201.

Abstract □ Amino acids methionine and histidine, which are soluble in propylene glycol, were investigated for their purported beneficial effects on aspirin-induced gastric mucosal damage in the rat. The pathognomonic changes observed microscopically in the fundic region of the stomach of animals administered daily doses (100 mg/kg), for up to 15 days, of aspirin solutions (0.36 M) in propylene glycol incorporated with the amino acids were compared with those of animals given equivalent quantities of aspirin in an aqueous suspension combined with an aluminum hydroxide antacid. A "delayed" onset of aspirin-induced cellular damage due to the presence of amino acids, analogous to that associated with the use of antacids, was found as determined partly by differences in the staining ability of injured cells with hematoxylin and eosin.

Keyphrases □ Methionine—effect on aspirin-induced gastric mucosal damage in rats □ Histidine—effect on aspirin-induced gastric mucosal damage in rats □ Aspirin—induction of gastric mucosal damage in rats, effect of methionine and histidine □ Amino acids—methionine and histidine, effect of aspirin-induced gastric mucosal damage in rats □ Gastric mucosal damage—induced by aspirin in rats, effect of methionine and histidine

GI bleeding in normal subjects, but especially in patients afflicted with chronic GI lesions, can accompany aspirin ingestion (1, 2). Several mechanisms reported for the pathogenesis of these lesions involve aspirin administration by the intra- or extragastric route (3–5). Among the more significant factors in aspirin-induced gastric hem-

0022-3549/79/0300-0295$01.00/0